



Article

Sediment Thickness Model of Andalusia's Nearshore and Coastal Inland Topography

Cristina Torrecillas ^{1,2,*} , Andres Payo ^{1,*}, Manuel Cobos ³ , Helen Burke ¹, Dave Morgan ¹, Helen Smith ¹ and Gareth Owen Jenkins ¹

- ¹ British Geological Survey, Keyworth NG12 5GG, UK; hbu@bgs.ac.uk (H.B.); djrm@bgs.ac.uk (D.M.); hsmith@bgs.ac.uk (H.S.); gjenkins@bgs.ac.uk (G.O.J.)
² Departamento de Ingeniería Gráfica, Escuela Técnica Superior de Ingenieros, Universidad de Sevilla, 41092 Seville, Spain
³ Department of Structural Mechanics and Hydraulic Engineering, Universidad de Granada, 18071 Granada, Spain; mcobosb@ugr.es
* Correspondence: torrecillas@us.es (C.T.); agarcia@bgs.ac.uk (A.P.); Tel.: +34-954486160 (C.T.); +44-(0)-115-936-3103 (A.P.)

Abstract: This study represents the first attempt to map the sediment thickness spatial distribution along the Andalusian coastal zone by integrating various publicly available datasets. While prior studies have presented bedform- and sediment-type syntheses, none have attempted to quantify sediment thickness at the scale and resolution performed in this study. The study area has been divided into 18 physiographic zones, and we have used BGS Groundhog Desktop v2.6 software for 3D modeling and sediment thickness model calculations. We present here the modeling workflow, model results, and the challenges that we have encountered, including discrepancies in geological maps, difficulty managing data input for grain size/consolidation, and the need for additional geological information. We have compared the modeled sediment fractions of the unconsolidated material with 4194 seabed samples distributed along the study area and found that the differences between the modeled versus the sampled emphasized the importance of incorporating river contributions, particularly from the Guadalquivir River, into the model for more accurate results. The model intermediate and final outputs and the software routines used to query the sediment thickness model are provided as publicly accessible datasets and tools. The modeled sediment thickness could contribute to making quantitative predictions of morphological change at a scale that is relevant to longer-term strategic coastal management in Andalusia. The methodology and tools used for this study are transferable to any study area.

Keywords: unconsolidated sediments; subsurface sediments; coastal modeling; coastal management; Groundhog Desktop



Citation: Torrecillas, C.; Payo, A.; Cobos, M.; Burke, H.; Morgan, D.; Smith, H.; Jenkins, G.O. Sediment Thickness Model of Andalusia's Nearshore and Coastal Inland Topography. *J. Mar. Sci. Eng.* **2024**, *12*, 269. <https://doi.org/10.3390/jmse12020269>

Academic Editor: João Miguel Dias

Received: 13 December 2023

Revised: 29 January 2024

Accepted: 30 January 2024

Published: 1 February 2024



Copyright: © 2024 by the authors. Licensee MDPI, Basel, Switzerland. This article is an open access article distributed under the terms and conditions of the Creative Commons Attribution (CC BY) license (<https://creativecommons.org/licenses/by/4.0/>).

1. Introduction

One of the most significant challenges facing coastal geomorphology and engineering today is to make quantitative predictions of morphological change at a spatiotemporal scale that is relevant to strategic coastal management [1–4]. The spatial scale might range from the local hydrodynamic to the wide sedimentary cell (10^2 to 10^4 m). The temporal scale is herein referred to as the mesoscale and is characterized by time horizons of the order of 10^1 to 10^2 years. The need for these quantitative assessments at the mesoscale has been reinforced by the 2019 Special Report on the Ocean and Cryosphere in a Changing Climate [5], which concluded that adaptation to a rise in sea level would be needed no matter what emission scenario is followed. As a response to rising sea levels, the location of the shoreline is anticipated to change, with the magnitude and direction of the change (transgression or progradation) being a continuum between two extreme behaviors: passive inundation and morphodynamical evolution. Passive inundation occurs when the land

surface is static during transgression, and therefore, shoreline retreat follows the slope of the backshore topography. Morphodynamical evolution is usually accompanied by erosion and deposition, which drive morphologic changes that impact future retreat. Which of these two extreme behaviors is more likely to occur can be understood from knowledge of the nearshore and coastal inland topography and shallow sub-surface sediment concentration [6,7].

The nearshore and its coastal and inland topography and sub-surface sediment concentration can be characterized using different parameterizations. For example, [8] used a simple geometrical analysis of the nearshore and backshore topography to assess the likely response of any wave-dominated coastline to a sea-level rise, and we applied it along the entire coastline of Great Britain. This work illustrated how the backshore geometry can be linked to the shoreline response (rate of change and net response: erosion or accretion) to a sea-level rise by using a generalized shoreline Exner equation, which includes the effect of the backshore slope and differences in sediment fractions within the nearshore. Another approach is using a more detailed numerical simulation platform such as the Coastal Modeling Environment (CoastalME) [9]. CoastalME is a modeling framework for coastal mesoscale morphological modeling that can produce close linkages between the scientific model abstractions and more realistic visualizations [10] in the form of lines, areas, and volumes, and the 3D representation of topographic and bathymetric surfaces and shallow sub-surface sediment composition. In CoastalME, the nearshore and inland coastal topography and sub-surface are conceptualized as a sediment thickness model, which is supplied as a set of raster files. The CoastalME parameterization, as a Sediment Thickness Model (STM), has been applied along sections of the east coast of England [11,12] and at sections of the south coast of Spain (Region of Andalusia) [13,14].

The Andalusian coastal zone is an area that will benefit from a holistic assessment of coastal sediment availability and spatial distribution at a scale that is relevant to longer-term strategic coastal management. According to the study by Molina et al. [15], in the 1956–2006 period, an erosion rate of nearly $-30 \text{ m}^2/\text{year}$ was observed in 28 zones out of 47 zones in total. Additionally, the European Environment Agency assessed Andalusia as a vulnerable region with erosion along 37% of its coastline [16]. The construction of coastal defense hard structures, such as seawalls, revetments, groins, and breakwaters, or even ports, harbors, and marinas, have indirectly contributed to coastline armoring [17], reducing the amount of sediment available in the nearshore. Not so obvious is the shore retreat induced by the construction of dams, which further limits the sources of sediment that feed the coast [18].

The aim of this work is to create an STM for the entire Andalusian nearshore and coastal inland region (see Figure 1) in a format that is suitable to simulate mesoscale coastal change using CoastalME. To build this STM, we have followed the FAIR (Findability, Accessibility, Interoperability, and Reusability) guiding principles for scientific data management and stewardship [19]. We have placed special emphasis on using publicly available data and documenting any transformation performed during the modeling process to allow data users to trace back to the original geological and topographical data used. This manuscript is organized into five sections, starting with the material and methods section and a brief introduction to the study site, data sources used flowchart, and a description of the BGS Groundhog Desktop software (v2.6) [20,21] utilised to generate the STM of Andalusia (STMA). The results section is divided into the five Andalusian provinces with coastal zones (Huelva, Cádiz, Málaga, Granada, and Almería, see Figure 1). For each province, we present the interpreted sections used to build the 3D lithological model and how, by combining this with an assessment of the percentages of the different sediment fractions, the STMA model is obtained. In addition, for validation purposes, we have tested the model along the coast and checked it against superficially sampled points. In the discussion section, we present model results the challenges encountered and outline possible future improvements to both the workflow and the Andalusian STM created.

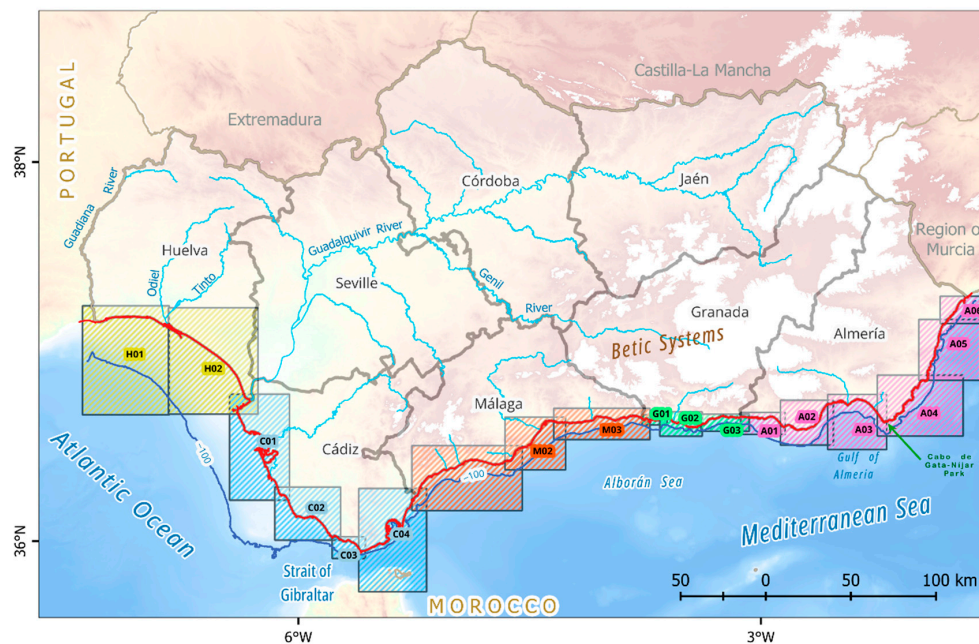


Figure 1. Study area with 18 zones based on colored provincial delimitations. Each zone label starts with the first letter of the province name, e.g., Huelva zones begin with H and Cádiz with C. The Andalusian coastline is represented as a red line with main rivers and -100 m bathymetric contour (EMODnet) in blue lines. Provincial boundaries are shown with a wide grey line. The background is the Mean depth Web Map Service from EMODnet release 2020 [<http://ows.emodnet-bathymetry.eu/ows> (accessed on 9 November 2023)]. This map and the following maps use EPSG 25830 coordinates with a geographical coordinates grid.

2. Background and Ancillary Data Used

2.1. Study Area

Andalusia is one of the 17 regions that make up Spain. It is located on the south of the Spanish peninsula; to the east, it borders the Region of Murcia; to the west with Portugal; to the north with the regions of Extremadura and Castilla-La Mancha; and to the south with the Atlantic Ocean, the Mediterranean Sea, and the Strait of Gibraltar (see Figure 1). In 2022, this region was the most populated in Spain, with 8,500,187 inhabitants (17.8%) [22] and the second largest area with 87,268 km² (17.4%). The coast stretches for 1200 km, measured at a scale of 1:25,000, and traverses five of its eight provinces, which from west to east are Huelva, Cádiz, Málaga, Granada, and Almería. It is an economically important region [23], and in 2021, 37.4% of the Andalusian population will live within 10 km of the coast (4.5% of the entire Andalusian territory) [24]. Furthermore, Andalusia has established itself as one of the main tourist destinations in Spain, with a total of 30.9 million tourists in 2022, almost 50% of whom visited the sunny and sandy coast of Málaga or Cádiz [25].

The coast of Andalusia is characterized by a wide variety of geomorphological features, including coastal plains, rugged cliffs, sandy beaches, and several coastal mountain ranges [26]. It is composed of three clearly differentiated areas: (i) a western sector up to the Strait of Gibraltar, exposed to significant ocean swell from the Atlantic Ocean (fetch), with a mesotidal character and a prevalence of sandy formations, estuaries, and tidal marshes; (ii) the Strait of Gibraltar where the exchange of bodies of water between the Mediterranean Sea and Atlantic Ocean occurs; and (iii) the eastern sector (Mediterranean sea), exposed to weaker waves, microtidal, and with a higher presence of rocky and cliffed coastlines, along with narrow beaches, deltas, and lagoons. Its bathymetric geomorphology has different marine platform widths between the Atlantic Ocean and the Mediterranean Sea coast, as is exposed in Figure 1, which represents a -100 m bathymetric contour. The seabed in the Atlantic provinces (Huelva and west of Cádiz) has an extensive and gently sloping continental shelf extending over 40 km to reach a sloping seabed with a depth of

100 m, in contrast to the Mediterranean provinces with gradual slopes leading to deeper water (offshore platform) reaching 80 m in only 4 km (Málaga). Therefore, the influence of rivers such as the Guadalquivir or Guadiana (Figure 1) has resulted in the formation of extensive estuaries, pro-deltas, and marshlands along the coast [27]. Much of Andalusia's coastline is composed of marine sediments deposited during a time of higher sea levels in the Neogene [28]. In the Mediterranean coastal areas, especially in the regions of Almería and Málaga, limestone and schist cliffs rise majestically above the sea [29].

2.2. Data Input

The topo-bathymetry and shallow subsurface geological data are required as input data to create an STM. For these data sets, we have used the same geospatial reference system, ETRS89 geodetic system, and 30N UTM projection (EPSG 25830), and adequate spatial resolution or cell size for the study (between 25 and 100 m). The sources of the dataset and a brief description of each data included are summarised here:

- One Seamless Topo-bathymetry model (STBM) for each zone. This dataset is a raster mosaic divided by 18 zones (see Figure 1). Each zone was compiled by mixing topographic and bathymetry data and filling in and interpolating the gap areas. The geodata sources in this dataset were:
 - Topography: the elevation was obtained from the Digital Terrain Model (DTM) with a 25 m grid pitch obtained by interpolation of 5 m-cell size DTM from LiDAR 2014–2015 flights, in Spanish called MDT25 and distributed by the Spanish National Center for Geographic Information (CNIG, in Spanish Centro Nacional de Información Geográfica) [30].
 - Bathymetry: For the seabed, two main datasets were collected. In shallow water, several Eco bathymetries (ECOBAT) were downloaded in ESRI shape format from the Andalusian environmental network website called REDIAM (in Spanish, RED De Información Ambiental de Andalucía) [31]. They were mapped with bathymetric contours at 1:1000 (Cádiz, Granada, and Almería) and 1: 5000 (Málaga) scales between 2008–2012 [32]. They cover the whole Andalusia coastline (<100 m depth), except the Huelva shoreline, and were interpolated to obtain a continuous GeoTiff format. In Huelva and deep waters, the F3 and F4 tiles from the DTM 2020 product by EMODnet Digital Bathymetry were collected [33].
 - Physiographic zones: Due to the extension of the coast and its wide geomorphology, 17 (18 at the end) physiographic zones were defined. They were based on the orientation of the coastline, the shape of the continental shelf, river intersections, headlands, the main sediment type, and the level of influence from atmospheric and maritime weathering agents.
 - Coastline: The topographic and bathymetric datasets were joined using an additional vectorial layer as the limit between land and sea. The layer was downloaded for each province from the REDIAM website [34].
 - Seabed sediment samples and Granulometric curves: During ECOBAT, field surveys obtained more than 4500 samples of seabed sediments in the study area [32]. This information is used to control the quality of the model. The percentage of fine (<0.063 mm), sand (>0.063 mm and <2 mm), and gravel (>2 mm) material, according to the sediment type division in our STM for each point, was obtained from the granulometric curves.
- Subsurface. This dataset is composed of two main subsets:
 - Geology: 25 Geological maps at a scale 1:50,000 (MAGNA 50) were downloaded from the Spanish Geological and Mining Institute website (IGME, in Spanish for Instituto Geológico y Minero de España) [35]. These maps also include the stratigraphic order, schematic boreholes, and cross-sections.
 - Geomorphology: One Seafloor sediment polygon shape layer (SEASED) from the digitalization produced by the Andalusian Government of the Geomorphologic

Map of Spain and the Continental Margin at scale 1:1,000,000 compiled by IGME and other institutions and distributed by REDIAM [36] was used as complement information in the definition of the seabed unconsolidated sediments.

3. Methodology

3.1. STMA Elaboration

Figure 2 illustrates the overall workflow followed to produce the STMA. The methodology is similar to the one used by [12] and starts by building an STBM from the geospatial information in Section 2.2. Once the free information was downloaded, all information was exported in GeoTiff format, so an exportation (DTM2020) or raster interpolation over vectorial contours data (ECOBAT) was carried out in a GIS environment (QGIS software v3.28.1). Additionally, the official assignment of the coordinate system in ETRS89 and UTM zone 30 (EPSG 25830) required geodetic transformations (in the case of WGS84 datum) or the application of the UTM projection for geographic coordinates or change zone 29 to 30 (29N is used in west Andalusia). The next step was the creation of raster mosaics with a previous analysis of 0 m level and filling of the gaps between elevations and depths using piecewise linear interpolations. The interpolant is constructed by triangulating the input data with a convex hull and, on each triangle, performing linear barycentric interpolation [37]. The nearshore region is interpolated using unstructured spatial data, while the deepest regions and the land side are interpolated with structured spatial data. Seventeen overlapping physiographic zones were defined based on the generalization of a coastal characterization vector layer, and the mosaics were clipped by these boundary boxes. Additionally, a spatial resolution was allocated to each zone based on its area dimensions to equalize the number of pixels within each zone. Only the Huelva zones (H01 and H02 in Figure 1) do not overlap, which responds to a necessary subdivision to reduce the maximum number of raster cells imposed by the postprocessing Groundhog software v2.6 [21]. Therefore, a total of 18 combined zones represent the STMB dataset for the whole study area.

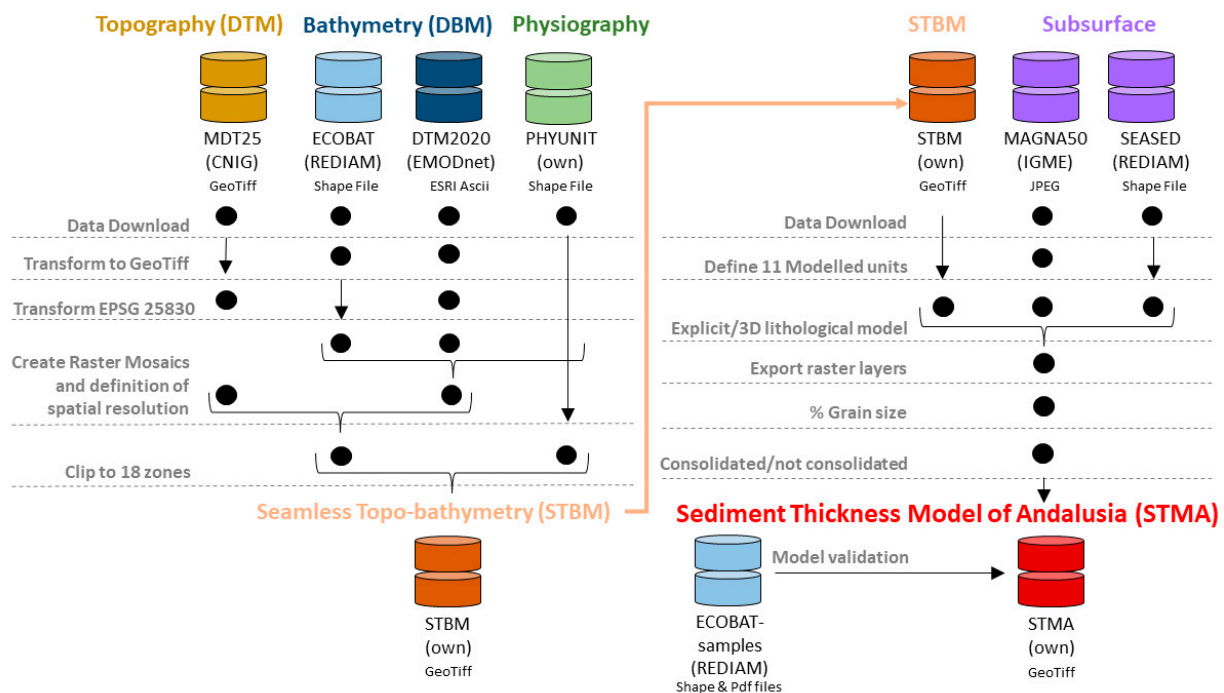













Figure 2. Workflow diagram showing the data used and main steps followed to create the Sediment Thickness Model of Andalusia (STMA).

These raster mosaics are then combined with the subsurface to produce, firstly, a 3D geological model of the Quaternary sediments and, finally, the STMA. The 3D geological

model was generated by combining the STMB as the top layer, geological information from MAGNA50 (consisting of a geology layer, schematic boreholes, stratigraphic order, and cross-sections included as additional information in raster sheets) and the seabed sediment layer (SEASED). Previously, a simplification and harmonization of geological units to eleven was carried out by combining units of similar age and lithology (Table 1).

Table 1. Eleven modeled units with lithology, grain size proportions, and degree of consolidation based on geological map descriptions.

Color	Modeled Unit	Lithology	% Fine	% Sand	% Gravel	Consolidated/ Unconsolidated
	Beach and dunes	Holocene beach deposits and sand dunes	5	85	10	Unconsolidated
	Holocene silts and clays	Holocene estuarine silts and clays	95	5	0	Consolidated
	Slope deposits	Loose sand and gravel on steep slopes	33	33	34	Unconsolidated
	Older silts and clays	Silts and clays at higher elevations and further inland	95	5	0	Consolidated
	Marine clay	Offshore seafloor clay ¹	100	0	0	Unconsolidated
	Marine sand	Offshore sand deposits ¹	0	100	0	Unconsolidated
	Marine gravel	Offshore gravel deposits ¹	0	0	100	Unconsolidated
	Pleistocene sands	Older sand deposits	0	95	5	Consolidated
	Conglomerate	Cemented sand, gravel, and cobbles	0	90	10	Consolidated
	Weak rock	Limestone/mudstone	0	0	100	Consolidated
	Strong rock	Volcanic and crystalline basement rocks	0	0	100	Consolidated

¹ Assumed age/stratigraphy for offshore deposits.

All this information enables the geologist to construct cross-sections using schematic boreholes for guidance and the mapped outcrops to produce a geological fence diagram. Interpolation between the nodes along the drawn sections and the limits of the units produces a solid model comprising a stack of triangulated objects, each corresponding to the base of one of the geological units present. For the interpolation of the 3D geological model, we used Groundhog Desktop v 2.6 software [21], see Figure 3. This software was developed by the British Geological Survey (BGS) to visualize, model, and interpret geological and environmental data. Then, the elevation difference between the top and base of each geological unit (i.e., its thickness) is calculated by triangulating between digitized nodes along the cross-sections and nodes around the edges of unit coverages digitized from the geology maps. This modeling methodology required the definition of (i) Individual model for each physiography area, (ii) Modeled to ca. 1.5 km inland, (iii) Section spacing 1–2 km inland/nearshore, less detailed offshore, and (iv) Model cut off depth in –30 m onshore and 5 m offshore.

The resulting sediment thickness models were then exported as grids with a user-defined cell size for each physiography area. In line with the model’s original purpose (input data in CoastalME) [9], this cell size was adjusted to ensure that each raster did not exceed a certain number of cells and the distance between the wave breaking point and the coastline was represented by at least four or five cells in this spatial resolution.

The next step was the estimation of the percentage of grain size in Fine (F), <0.063 mm, Sand (S), >0.063 mm and <2 mm, and Gravel (G), >2 mm, and interpretation of the mechanical state as either consolidated (C) or unconsolidated (U) for the three grain sizes. The size fractions within a layer are assumed to be well mixed. Any of these size fractions may be omitted for some or all raster cells, in which case the model will assume zero thickness of this size fraction for that raster cell. Consolidated sediments are essentially solid rocks composed of materials that have been metamorphosed or cemented together, such as sedimentary rocks, including conglomerate, sandstone, siltstone, shale, and limestone. Unconsolidated sediments are loose materials ranging from clay to sand to gravel. The

grain size proportions and the consolidated/unconsolidated state were based on expert interpretation of the lithological descriptions on the maps (Table 1). At the end of this process, the STMA is obtained and is composed of six layers: three for C material and three for U material with the thickness of F, S, and G sediments for each study zone and saved as a Grid file (Geotiff).

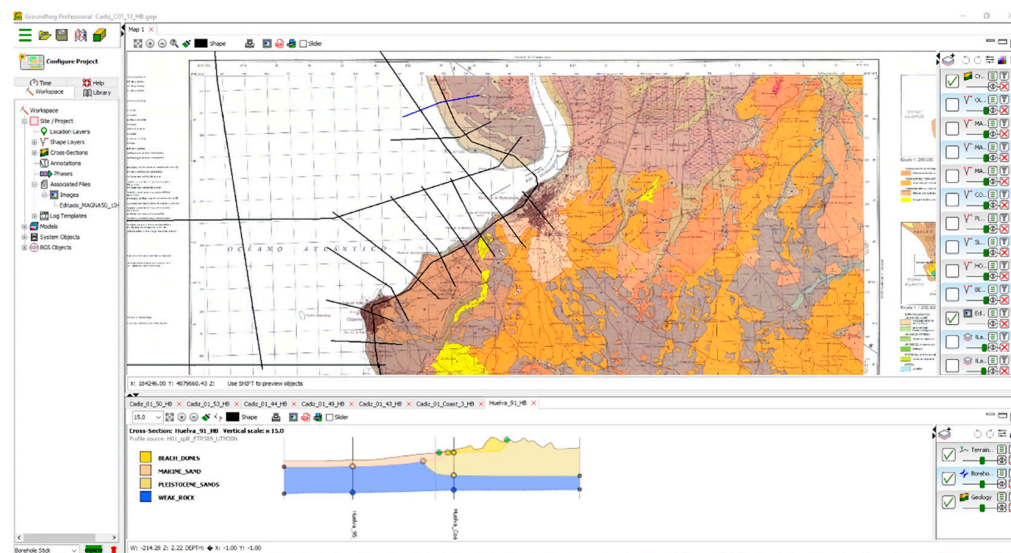


Figure 3. Screen capture of BGS Groundhog Desktop software v2.6 environment showing a zoomed view of Huelva province. Geological map shown in colors, cross sections shown as black lines in plan-view and detailed cross section of the selected cross section (blue line) shown in bottom panel.

3.2. Model Querying Tools and Validation

STM is not only one of the main input files for coastal landscape dynamical simulation within CoastalME but can also be queried in different ways to produce information that is useful for coastal engineers and stakeholders. To illustrate how this can be done, we have developed three types of geospatial querying approaches for STMA: full area, area-specific, and point sample querying. Each of these querying approaches has been implemented in six scripts and models in the QGIS environment using Pyqgis language and its own Model designer [38]. There are three Pyqgis scripts: (i) to add the STMA to QGIS grouping the layers by province and zone (1_Add_STMA_by_province_and_zone.py); (ii) to add STMA value to a point sample layer (2_Point_value_STMA.py); and (iii) to calculate the zonal statistics of a polygon area (3_Zonal_statistics_STMA.py). For the visual macro models, there were also three to calculate: (i) Volume of each material in one zone (1_Volume_STMA.model3); (ii) Volume of each material in a clip area using a polygon layer (2_Volume_STMA_Clip.model3) and (iii) Zonal statistics of a polygon area (3_Zonal_statistics_STMA.model3), this last one is a model version of the last Pyqgis script 3_Zonal_statistics_STMA.py. The first two models could be used in batch processing if the user needs information on more than one zone. They can be accessed on the same data repository where the STMA data is publicly available (see data availability statement).

These programs have been used to analyze and validate the model as a final stage. In this way, some calculations were carried out to test the STMA and gain a better understanding of the results (e.g., raster sums or volume calculations). Additionally, as a quality control, we utilized ca. 4500 sample points of seabed sediments gathered as part of the ECOBAT project. We specifically chose samples that overlapped with the STMA and calculated the differences between the unconsolidated sediments model predictions and the actual samples.

4. Results

In this section, we first present a general overview of the results, followed by a summary of the main assumptions and simplifications performed to create the STMA. We also highlight the challenges encountered in each province, together with a brief description of the resulting STMA and the query and validation of the model with quality control. Both the STMA and the QGIS utilities used to extract the information presented in this section are available in a publicly accessible repository.

The 18 zones on which the whole of Andalusia’s STM were divided and mapped by a team of four geologists, who oversaw Huelva, Cádiz, Málaga-Granada and Almería, respectively. To cover the whole study area, we have produced more than 830 profiles (see Figure S1), which represent a total of 7225 km of interpreted shallow subsurface sections. For each of the 18 rectangles, we have created six layers of Consolidated and Unconsolidated Fine (CF and UF), Sand (CS and US), and Gravel (CG and UG) material. The resulting sediment thickness models for each zone and each one of the six layers are shown in Figures 4 and 5. The spatial resolution or cell size of each zone, its number of cells, and mean, median, minimum, and maximum value of thickness are shown in Table 2. In both elements, it is evident that the sediment thickness of the arbitrarily chosen bottom layer (CG) is the largest, as expected, in all divisions and on the order of 1000s of meters, and the remaining five layers have a thickness that varies from a few meters to 100s of meters.

Table 2. Cell size, number of cells, Median, and Mean of thickness of the different STMA zones in alphabetic order.

Zone	Cell Size (m)	Num. of Cells	Grain	Unconsolidated				Consolidated			
				Mean (m)	Median (m)	Min (m)	Max (m)	Mean (m)	Median (m)	Min (m)	Max (m)
A01	50	522 × 258	F	149.5	117.1	0.0	877.9	1943.0	1992.8	0.0	2096.2
			S	3.3	0.0	0.0	106.7	0.0	0.0	0.0	1.1
			G	0.0	0.0	0.0	7.7	1864.3	1903.5	1533.8	1912.8
A02	50	623 × 527	F	134.3	163.7	0.0	370.2	67.6	0.0	0.0	1095.3
			S	0.2	0.0	0.0	23.8	3.6	0.0	0.0	57.6
			G	0.0	0.0	0.0	2.8	1864.6	1870.0	0.0	2064.5
A03	50	692 × 648	F	86.2	16.1	0.0	1804.8	17.2	0.0	0.0	799.9
			S	0.7	0.0	0.0	55.0	0.9	0.0	0.0	42.1
			G	0.0	0.0	0.0	1.8	1772.4	1877.3	0.0	1993.7
A04	100	504 × 358	F	238.7	100.2	0.0	1960.4	28.3	0.0	0.0	614.8
			S	84.8	0.0	0.0	1621.4	1.5	0.0	0.0	32.4
			G	0.0	0.0	0.0	2.9	1275.5	1410.2	0.0	1873.3
A05	50	726 × 716	F	104.2	13.8	0.0	410.1	29.3	0.0	0.0	840.8
			S	0.0	0.0	0.0	39.8	1.5	0.0	0.0	44.3
			G	47.6	0.0	0.0	322.6	1284.7	1453.8	0.0	1787.7
A06	50	570 × 320	F	173.0	179.0	0.0	720.8	0.3	0.0	0.0	383.2
			S	0.0	0.0	0.0	15.6	0.4	0.0	0.0	1601.2
			G	0.0	0.0	0.0	1.8	1601.0	1788.7	0.0	1975.9
C01	75	472 × 831	F	0.3	0.0	0.0	10.9	0.0	0.0	0.0	9.5
			S	1.3	0.0	0.0	44.1	3.5	0.0	0.0	2499.7
			G	0.0	0.0	0.0	5.6	2040.3	2035.4	1962.1	2182.6
C02	50	780 × 630	F	0.0	0.0	0.0	12.4	0.0	0.0	0.0	5.9
			S	1.3	0.0	0.0	240.9	0.2	0.0	0.0	55.4
			G	0.1	0.0	0.0	18.3	2059.8	2055.2	1943.2	2481.7
C03	25	780 × 508	F	0.1	0.0	0.0	35.1	0.0	0.0	0.0	0.0
			S	4.3	0.0	0.0	97.6	0.0	0.0	0.0	28.7
			G	0.0	0.0	0.0	6.9	1995.6	2017.3	0.0	2524.5
C04	100	399 × 607	F	2.0	0.0	0.0	112.9	0.1	0.0	0.0	304.4
			S	2.4	0.0	0.0	412.7	0.0	0.0	0.0	16.0
			G	0.1	0.0	0.0	84.2	1893.2	2024.5	1073.9	2866.7

Table 2. Cont.

Zone	Cell Size (m)	Num. of Cells	Grain	Unconsolidated				Consolidated			
				Mean (m)	Median (m)	Min (m)	Max (m)	Mean (m)	Median (m)	Min (m)	Max (m)
G01	25	592 × 240	F	0.0	0.0	0.0	0.3	0.2	0.0	0.0	22.0
			S	0.0	0.0	0.0	0.7	0.0	0.0	0.0	1.2
			G	4.4	1.0	0.0	2040.4	2068.4	2021.3	0.0	6403.3
G02	25	996 × 575	F	0.9	0.0	0.0	71.7	2.0	0.0	0.0	91.6
			S	0.0	0.0	0.0	1.6	0.1	0.0	0.0	11.6
			G	1.8	0.0	0.0	2049.2	2034.6	1997.0	0.0	2956.0
G03	25	1140 × 399	F	296.4	300.8	0.0	867.7	0.0	0.0	0.0	1.9
			S	15.9	16.3	0.0	45.7	0.0	0.0	0.0	387.8
			G	0.0	0.0	0.0	1.9	1650.5	1653.2	0.0	1724.3
H01	100	510 × 640	F	10.4	7.1	0.0	99.0	0.3	0.0	0.0	25.8
			S	6.9	0.0	0.0	95.3	1.0	0.0	0.0	13.1
			G	0.5	0.0	0.0	24.8	1875.8	1959.7	1474.9	2031.1
H02	100	525 × 625	F	24.7	10.7	0.0	135.4	0.0	0.0	0.0	23.4
			S	2.5	0.0	0.0	91.3	0.0	0.0	0.0	28.1
			G	8.8	9.2	0.0	28.8	2013.5	2019.9	1878.6	2048.8
M01	100	648 × 381	F	0.0	0.0	0.0	9.0	0.0	0.0	0.0	6.4
			S	0.0	0.0	0.0	27.8	0.0	0.0	0.0	4.7
			G	0.0	0.0	0.0	9.2	1935.9	1972.1	1099.7	3478.8
M02	100	356 × 310	F	0.0	0.0	0.0	2.0	58.8	0.0	0.0	1067.2
			S	5.4	0.0	0.0	132.6	7.3	0.0	0.0	2509.0
			G	0.0	0.0	0.0	3.9	1945.4	1997.5	0.0	2146.2
M03	100	566 × 184	F	0.0	0.0	0.0	6.8	68.0	0.0	0.0	966.8
			S	0.3	0.0	0.0	116.0	3.6	0.0	0.0	50.9
			G	0.0	0.0	0.0	13.6	1943.0	1992.8	0.0	2096.2

4.1. Huelva

The province was divided into two zones. H01 is delimited to the west by the Guadiana River and east by the Tinto and Odiel rivers, while H02 is delimited to the east by the Guadalquivir River (Figure 1). The physiographic zones define a rectangular area of interest with a longer dimension oriented parallel to the coastline (West–East) that extends up to 50 km offshore due to the wide and shallow continental shelf in this region (Figure 1).

The topo-bathymetry was a composition of MDT25 and DTM2020 datasets. The link between the two data surfaces was supported by the layer containing the coastline. Landward and seaward, the topographic and bathymetric maps were used correspondingly.

The simplification and harmonization of geological units were complicated. In the case of Huelva, covered with five geological map sheets (998, 999, 1033, 1047, and 1033C); initially, 39 geological units (Unit code) were reduced to eight modeled units (Table 3) according to the eleven displayed in Table 1. The harmonization of geological units used for Huelva was also used for Cádiz, Málaga, Granada, and Almería.

The Quaternary deposits in the western half of Huelva are dominated by estuarine sediments (modeled as Holocene_Silts_Clays) associated with the river Odiel and its tributaries. Sand dunes and beach deposits (modeled as Beach_Dunes) are present along the entire Huelva coastline and are assumed to overlie the estuarine deposits. Offshore, the Huelva area is dominated by marine clay. The bedrock in the Huelva area is modeled as a weak rock.

The resulting STMA layers for the two Huelva zones, H01 and H02, are shown in Figures 4 and 5 as unconsolidated and consolidated sediments, respectively. Both physiographic zones are similar (Figure 4). Significant thicknesses in all unconsolidated sediments (135.4 m in H02 Fine, see Table 2) are observed, and the predominant consolidated sediment is the CG layer on the seafloor (more than 2000 m as mean in H02).

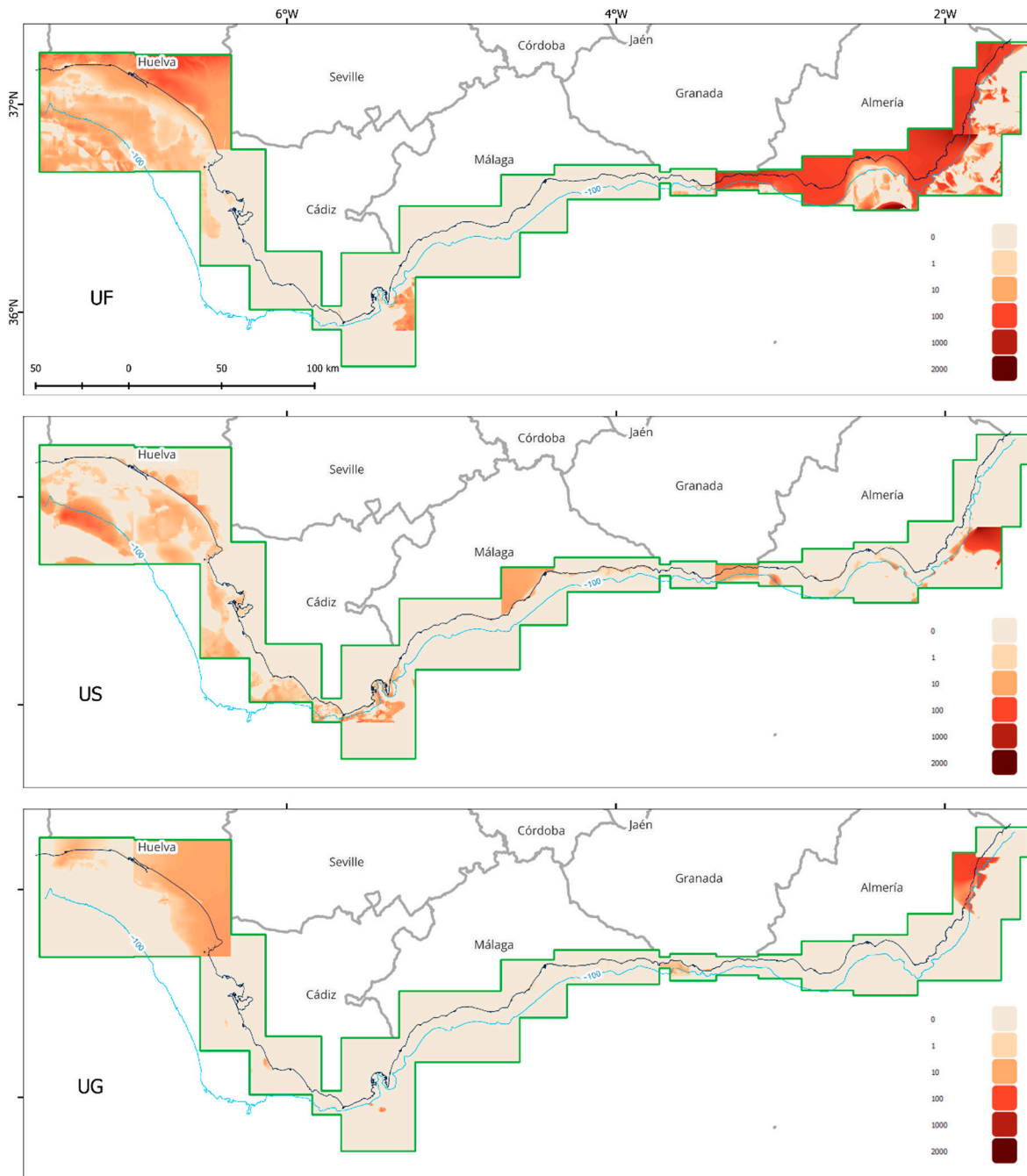


Figure 4. All three unconsolidated sediment thickness layers in meters that, combined, represent the STMA in the study area (green delimitation). From top to bottom, the three layers are Unconsolidated Fine (UF), Sand (US), and Gravel (UG). The Andalusian coastline is represented as a thin black line, and the -100 m bathymetric contour is represented as a blue line.

4.2. Cádiz

The physiographic zone C01 presents a flat morphology with a gentle slope and a wide continental shelf of approximately 35 km, as well as a continental slope with a somewhat gentler slope until its intersection with the abyssal plain. Starting from the west of C02, the width of the continental shelf is irregular, shortening, widening, and shortening again until almost disappearing at the eastern part of C03. From here, the coast is characterized by a rocky sector of cliffs of the flysch mantle, with a small or almost non-existent continental shelf along the Strait of Gibraltar to the Alboran Sea (C04, see Figure 1).

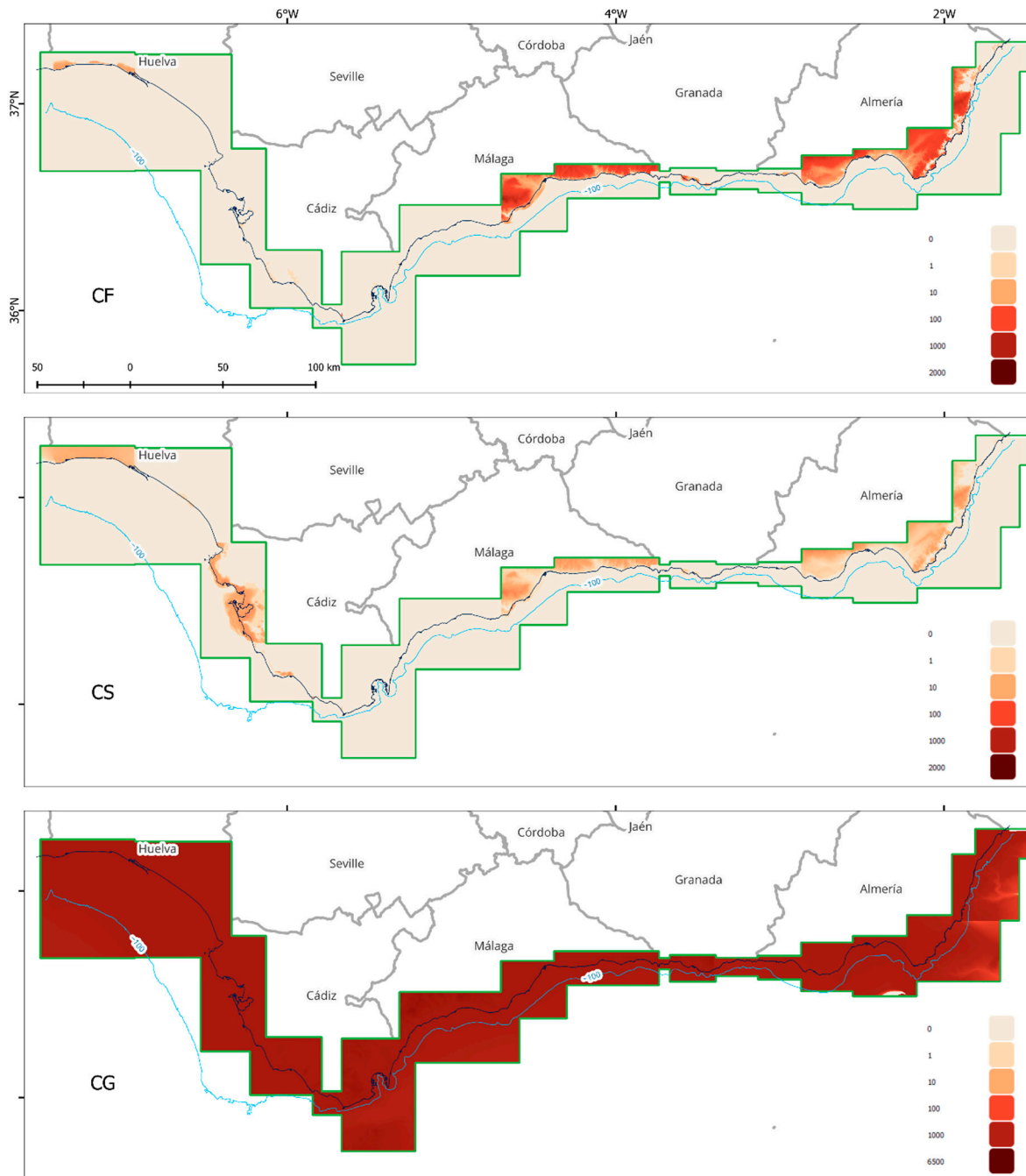


Figure 5. All three consolidated sediment thickness layers in meters that, combined, represent the STMA in the study area (green delimitation). From top to bottom, the three layers are Consolidated Fine (CF), Sand (CS), and Gravel (CG); note that the CG map uses a different upper boundary for the last division of the legend. The Andalusian coastline is represented as a thin black line, and the -100 m bathymetric contour is represented as a blue line.

As with Huelva, the map units were condensed into the same 11 modeled units, and a separate lithology/thickness model was constructed for each physiographic zone. The resulting STMA for the four Cádiz's zones, C01 to C04, are shown in Figures 4 and 5. The unconsolidated material follows the trend of the Huelva area, although the US increases its thickness to 412.7 m in C04 (Table 2). The consolidated material shows significant thicknesses in the CG layer up to 2524.5 m in zone C03 but not exceeding 500 m in other zones. C01 zone with CS presents thicknesses around 2500 m, including elevations inland.

Table 3. Mapped or modeled units for Huelva zones.

Map	Unit Code	Description	Modeled Unit
998	QD	Holocene white sands	Beach and dunes
998	QE	Holocene white sands	Beach and dunes
998	QG	Quaternary conglomerates and red clays	Beach and dunes
998	QM	Holocene silts, clays, and sands	Holocene silts and clays
998	QAI	Holocene sands and silts	Holocene silts and clays
998	TB/ CG-Q/2	Pliocene red clayey sands and gravels	Pleistocene sands
998	TB/21	Pliocene sandy silts and grey-yellow sands	Pleistocene sands
999	QP	Quaternary sand	Beach and dunes
999	QD2	Quaternary sand	Beach and dunes
999	Qt	Quaternary peat	Beach and dunes
999	QAI	Quaternary silts and sands	Holocene silts and clays
999	TB-2Q	Base Quaternary sands	Pleistocene sands
999	QT2	Quaternary gravels, sands, silts, clays	Slope deposits
1033	QP2	Quaternary sand	Beach and dunes
1033	QP1	Quaternary sand	Beach and dunes
1033	QAI	Quaternary silts and sands	Beach and dunes
1033	QD2	Quaternary sand	Beach and dunes
1033	QD	Quaternary sand	Beach and dunes
1033	TB-Q2	Pliocene sand	Pleistocene sands
1047	36	Holocene sands, pebbles, and shells	Beach and dunes
1047	32	Holocene sands	Beach and dunes
1047	31	Holocene sands, pebbles/cobbles and shells	Beach and dunes
1047	30	Holocene sand, poss dunes	Beach and dunes
1047	23	Holocene sands, pebbles/cobbles and shells	Beach and dunes
1047	10	Pleistocene/Quaternary quartz sands with some quartz and quartzite cobbles	Conglomerate
1047	12	Pleistocene conglomerate with carbonate-rich sandstone	Conglomerate
1047	7	-	Conglomerate
1047	19	Holocene greenish marls with hydromorphic soils (developed in waterlogged conditions)	Older silts and clays
1047	18	Pleistocene sand	Pleistocene sands
1047	16	Pleistocene sands and clays with carbonate cobbles	Pleistocene sands
1047	15	Pleistocene clayey sands with quartz cobbles	Pleistocene sands
1047	13	Pleistocene clayey sands with quartz cobbles	Pleistocene sands
1047	3	Tertiary siliceous white marls with radiolaria and diatoms (weak bedrock)	Weak rock
1033C	QP	Beach deposits	Beach and dunes
1033C	QT	Peat	Beach and dunes
1033C	QD2	Barrier dunes	Beach and dunes
1033C	QD1	Ancient dunes	Beach and dunes
1033C	QD	Aeolian sand	Beach and dunes
1033C	TB-Q2	Pliocene sand	Pleistocene sands

4.3. Málaga

From west to east, the first physiographic zone, M01, includes the three arcs formed by the western inlets of Málaga province (M01), which continues with a succession of coves until the city of Málaga at the east boundary of M02. After this, the orientation of the coast changes from SW-NE to E until its eastern limit with the province of Granada (M03). From west to east, a more pronounced bathymetric profile is observed, with a small continental shelf. This profile shallows slightly, leading to the development of a continental shelf of approximately 14 km in average length. The width of the platform fluctuates, with maximum widths found in the inlets, specifically in the Málaga inlet, where it reaches 20 km. The minimum width, approximately 6 km, is observed on the border with the province of Granada. The very high population along the coast is one of the main causes of the regressive behavior of its beaches. The Málaga coastline consists of an urban strip coinciding with a strip of low-altitude land (less than 10 km wide) that widens in the locations with a high-density population.

Overall, the coastline of the Málaga study area is predominantly composed of hard rocks from a wide range of geological eras, from Precambrian to Triassic igneous, metamorphic, and sedimentary rocks. Major valleys and embayments feature alluvial and estuarine deposits. Extensive deposits of Pliocene rocks (weak and unconsolidated muds, sands,

gravels, and conglomerates) cover much of the low-lying coastal zone around the eastern region of M01 and M02, respectively. Beach sands are abundant along the coastal strips in areas where there is a supply of unconsolidated sediment (i.e., Miocene, Pliocene, and Quaternary deposits composed of mud, sand, gravel, conglomerates, and breccias).

The generated STMA for the three zones in Málaga, labeled as M01 to M03, is illustrated in Figures 4 and 5, respectively. Although the US layer contains a discontinuity between M01 and M02 inland, the sea part is continuous. This aspect is transferred to the CF and CS layers. CS has the most important maximum thickness value at M02 with 132.6 m, and UG maintains values above 2000 m (Table 2).

4.4. Granada

The Andalusian Mediterranean coast is characterized by its location close to the mountainous areas of the Betic Systems, which is approximately limited to the north by the Guadalquivir River and by a short hydrographic network with steep slopes (Figure 1). The western area of G01 is composed of gravel and sand. The physiographic zone G02 is composed of sandy and longer sand and gravel beaches. The eastern area is characterized by a few sandy beaches and sand and gravel, mostly limited by agricultural land (G03). The continental shelf, whose width hardly exceeds 10 km, is dotted with submarine canyons that reach the coast, such as the Jolúcar canyon (in the middle of G02), in which the depth varies from its head at the coastline to 500 m in just over ca. 7 km [39].

Superficial deposits are composed of beach sands and gravels (coarse-grained), which are intercalated with gravels and sands inland, and silts and clays on the alluvial plains in the central area of G02; sand dominates the offshore deposits in the western and eastern areas (G01 and G03), and the western part of G03. The offshore deposits of G02 are composed mostly of silts and clays. Superficial deposits are absent offshore in the center part of G02 and to the west of and center part of G03, where hard rocks are exposed on the seabed. The superficial deposits are underlain by hard metamorphic basement rocks throughout the model area, except for the eastern part of G03, where weaker sedimentary rocks are exposed.

The STMA outcomes for the three zones in Granada denoted as G01 through G03, are depicted in Figures 4 and 5. All unconsolidated layers have noteworthy values in G02 and G03 (867.7 m in G03 UF), where there is a discontinuity in the thickness of UF and US. Consolidated material fits well within the province and with the lateral provinces with significant values up to 6400 m (Table 2) due to the Betic Systems elevations.

4.5. Almería

In the case of the coast of Almería, three key regions are found: A01 is structured in relation to the intensive agricultural occupation of greenhouses and where the coastline is in regression; A02, A05, and A06 focus on popular tourist areas (beaches) which are characterized by a continuous succession of sandy points and beaches, inlets and small coves of fine sand with anchorages; and A03 and A04, which includes the city of Almería and the municipalities around the Natural Park of Cabo de Gata-Níjar (see Figure 1), and is an important tourist destination due to the natural park. In A05, the offshore shelf of Almería has a very limited width with a rocky sea floor cut by numerous submarine canyons. It has an average width of 5 km, reaching 20 km in the Cabo de Gata area. On the eastern coast of Almería, there is an abrupt relief, while in the Gulf of Almería (Figures 1 and 6), there is a much gentler relief.

The oldest rocks that outcrop in the region are the Betic substratum (micaschists and quartzites) and Neogene volcanic rocks of the Cabo de Gata complex. The Neogene-Quaternary sediments in the Almería region are typically composed of conglomerates, sandstones, mudstones, limestones, and volcanoclastic deposits. More recent Quaternary deposits (Holocene) are typically composed of fluvial deposits, alluvial fans, slope deposits, salt pans, lagoons, travertines, deltas, dune fields, and beach deposits. Offshore, the marine sediments are predominantly composed of sand, typically extending up to 7 km offshore,

where the sediments transition to marine clay. Areas of gravel are present in the nearshore regions off Cabo de Gata and in the far north of the region.

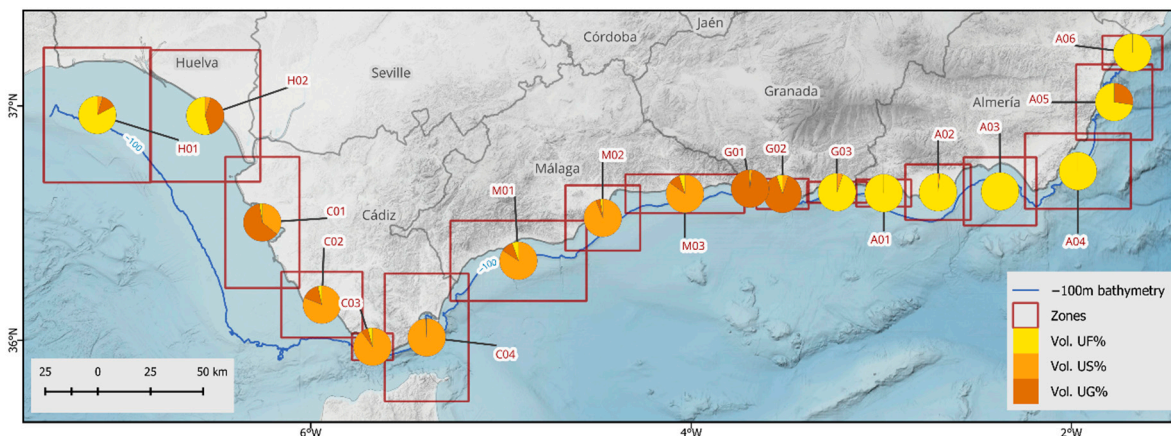


Figure 6. Pie chart of unconsolidated material volume along a 100 m-buffer coastline in each STMA zone: Unconsolidated Fine (UF), Sand (US), and Gravel (UG) sediments. The hillshade comes from the MDT25 XYZ tile service from Spanish IGN (<https://tms-relieve.idee.es/1.0.0/relieve/%7Bz%7D/%7Bx%7D/%7B-y%7D>, accessed on 9 November 2023).

The resulting STMA for the six Almería’s zones, A01 to A06, are shown in Figures 4 and 5, respectively. Figure 4 shows significant thicknesses of UF (maximum of 1960.4 m in A04, Table 2) and very localized minor areas of US and UG on the east coast. Meanwhile, the predominant consolidated sediment is the CG layer on the seafloor with less values than the rest of the study area in zones A01 (less than 400 m, Table 2).

4.6. Model Querying

Some queries were carried out along the coast to test the model and analyze its values. Firstly, the total thickness was calculated, and secondly, the volume of each type of unconsolidated material in each zone was evaluated.

The vertical sequence of the different sediment fractions (Fine, Sand, and Gravel) is not resolved in our model, but for consistency, we have assumed that the bottom layer is always the CG for all zones. Additionally, in all zones, the unconsolidated layers (UF, US, UG) are on top of the consolidated layers (CF, CS, CG). This has implications for the value of the sediment thickness of this bottom layer, as it is defined as the elevation between the arbitrarily selected baseline depth and the modeled surface of the CG at each location. We have chosen the modeling baseline depth of 2050 m, which represents the elevation difference between the current mean sea level position and the lowest elevation in the study area, which is located offshore of Almería province. The total elevation of any raster cell is obtained as the sum of the sediment thickness of all six layers, and, by definition, the expected values of total elevation along the shoreline are around the modeling baseline depth of 2050 m (see values in Table 4). The total elevation median and mean values vary between regions due to the different resolutions of the raster cells used at each region and due to the differences in steepness of the nearshore topography and bathymetry.

Figure 6 represents the pie chart percentage of UF, US, and UG volume along a 100 m- planimetric-buffer coastline for different physiographic zones extracted from the STMA. Percentages are calculated using only the unconsolidated layers for each zone (e.g., not representing the total sediment thickness). Table 4 presents the exact numbers. It represents the dominant sediment fraction size that will be found as you traverse the coastline of each zone. The values shown represent different lengths of coastlines, with H01 the largest at 53 km and G01 the shortest at 18 km. The results show how, near the delta and flatter inland regions of Huelva (H01), Granada (G03), and Almería (all ones less A05), the fine material dominates with more than 82% of the sediment thickness. In regions with

steeper inland relief (Cádiz, Málaga, and Granada, see hillshade in Figure 6), the dominant sediment fractions are sand and gravel, with fine fractions representing less than 6% of the sediment thickness.

Table 4. Median and mean elevation from −2050 m altitude reference along the coastline and Unconsolidated Fine (UF), Sand (US), and Gravel (UG) volume percentage in a 100 m-buffer coastline (200 m width) for each STMA zone.

STMA Zone	Median Elev. from Reference (m)	Mean Elev. from Reference (m)	%US	%UG	%UF
A01	2048	2048	0.17	0.02	99.80
A02	2051	2053	1.36	0.16	98.47
A03	2049	2052	0.18	0.01	99.79
A04	2060	2067	0.01	0.00	99.98
A05	2053	2060	0.03	27.31	72.64
A06	2055	2058	0.00	0.00	99.99
C01	2051	2051	35.66	61.93	2.40
C02	2049	2049	80.98	15.67	3.34
C03	2049	2050	89.86	6.15	3.98
C04	2054	2057	99.12	0.58	0.29
G01	2050	2054	1.73	97.39	0.86
G02	2049	2052	4.80	90.15	5.03
G03	2049	2052	5.09	0.00	94.90
H01	2051	2050	4.61	12.59	82.79
H02	2051	2051	4.83	40.94	54.22
M01	2052	2052	84.23	10.35	5.41
M02	2052	2053	94.00	3.99	1.99
M03	2050	2054	84.98	10.02	4.99

4.7. Model Validation

The validation process of the model involved comparing its values with sample points obtained from ECOBAT field surveys. These sample points were derived from granulometric curves found in a PDF file associated with the ECOBAT project. Unfortunately, there were no sample points available for the Huelva zones, as this area was not covered by the ECOBAT project. We selected points that overlapped with the study area, and in cases of overlapping zones, both differences were considered. Additionally, due to variations in cell sizes, some zones encompassed more than one measure (10.6% of cases), with only seven cells having 10 measures. In such instances, a mean value was computed. The final set of test points comprised a total of 4194 data points.

Figure 7 shows the percentage of unconsolidated sediment from ECOBAT samples. That percentage is calculated as the proportion between the thickness of a given unconsolidated layer and the thickness of the sum of unconsolidated layers, i.e., fine sand and gravel. The UF is mainly present in the eastern part of Granada, Almería, and offshore of Cádiz, where more than 80% of thickness layers are fine. Between 20% and 40% of fines are found at the mouth of the Guadalquivir River. The US covers the Andalusian coastline except for Almería. The percentage decreases from Cádiz (>80%) to Granada (~50%). The presence of UG in ECOBAT samples remains consistently low, concentrated primarily in Málaga, whereas Almería and Cádiz do not exhibit clear spatial concentrations.

The differences between ECOBAT samples and STMA are illustrated in Figure 8. Since these samples primarily pertain to surface sediments, the testing was limited to unconsolidated sediments. Discrepancies in locations between UF and the US are noticeable, particularly along the Almería and eastern part of the Granada coastline and in the western region near the mouth of the Guadalquivir River, where UG also exhibits elevated values. However, the median value in UF differences is low, as the boxplot shows. It is important to note that this version of STMA does not account for the additional sediment input from these rivers after the date of geological mapping around 1970, which contributes to the observed discrepancies. Among the components, UG yields the best results, which is

evident from the fewer instances of small differences and the lower variance in the box plot. In addition to this, the median value of UG is the lowest. Conversely, unconsolidated sand, especially influenced by large samples in the Guadalquivir River mouth, exhibits less favorable results. STMA indicates high percentages of Fine in Almería and the eastern part of Granada, contrary to ECOBAT samples that identified sand in those areas (refer to Figure 7 for UF and US).

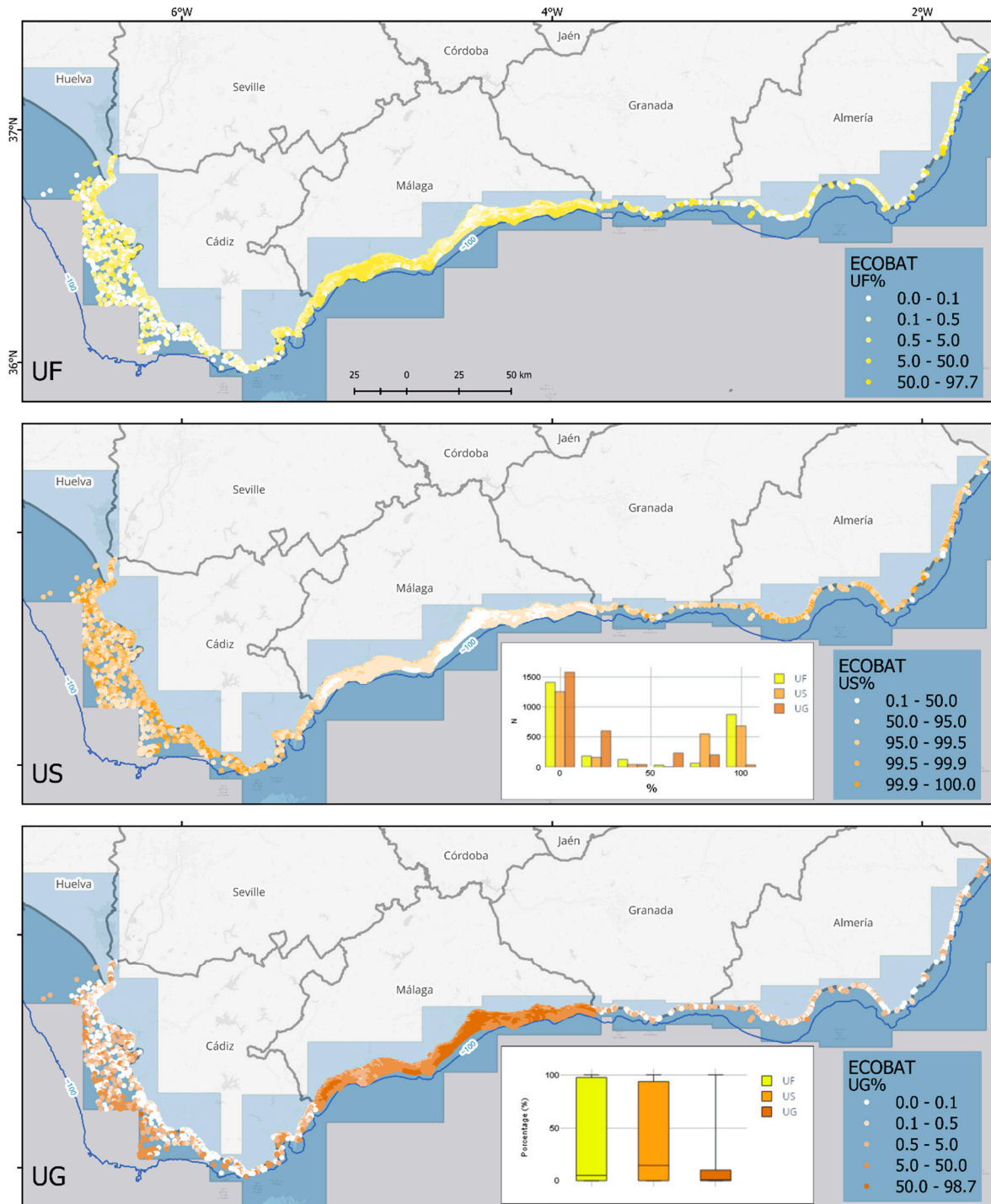


Figure 7. Percentage of unconsolidated sediment from ECOBAT samples. From top to bottom, the three layers are: Unconsolidated Fine (UF), Sand (US), and Gravel (UG); note that the US map uses opposite divisions in the legend. The figure below includes a boxplot of each ECOBAT sediment in percentage. STMA area is represented in blue.

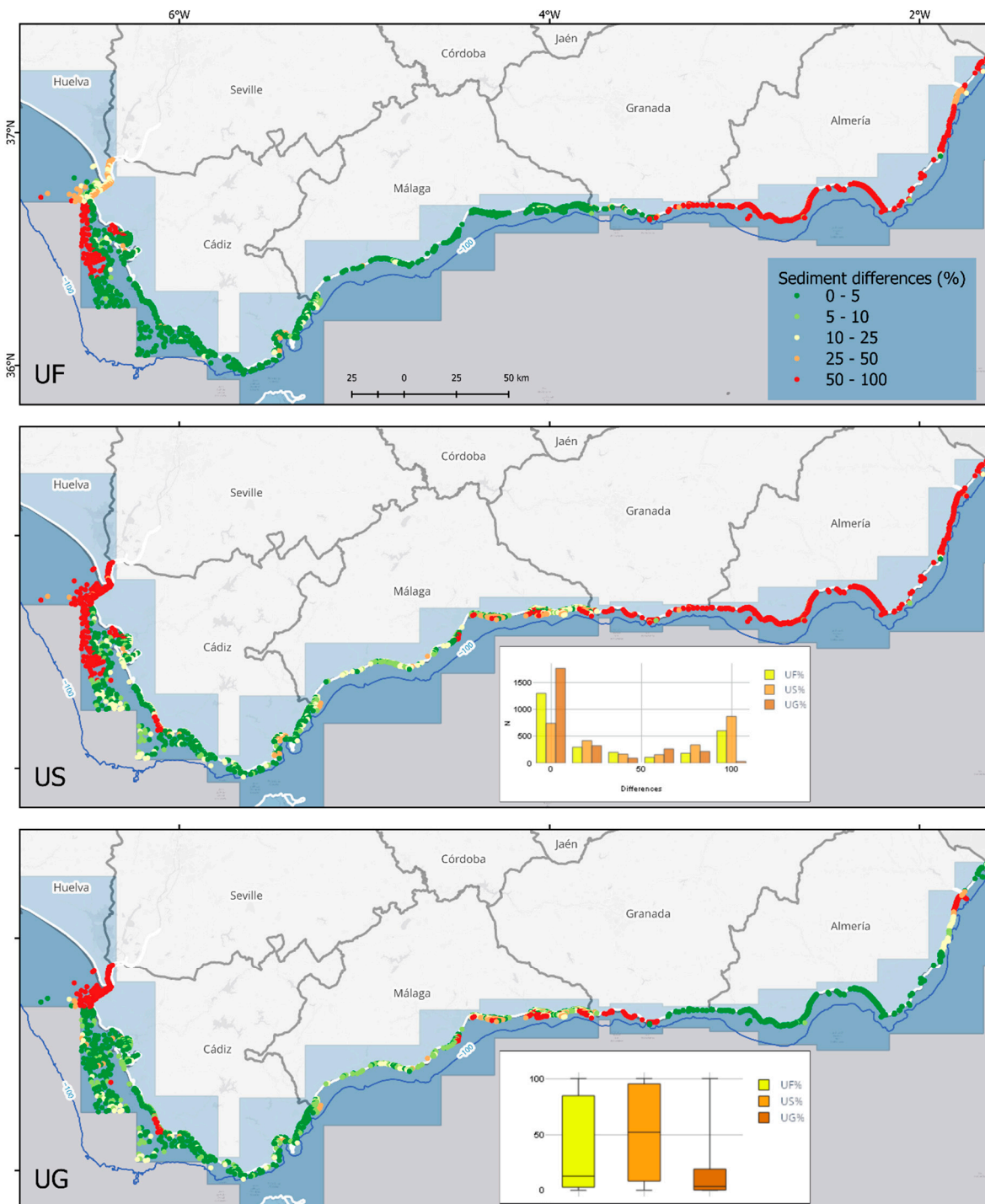


Figure 8. Percentage of sediment differences between STMA and ECOBAT samples. From top to bottom, the three layers are: Unconsolidated Fine (UF), Sand (US), and Gravel (UG). The US figure includes a histogram of the differences, and the UG figure is a boxplot of each sediment difference in percentage. STMA area is represented in blue.

5. Discussion and Conclusions

This study is the first attempt to map the thickness of the different sediment fractions along the Andalusian coastline by integrating geological, geomorphological, bathymetrical, and sedimentological datasets. The closest study performed to date was performed by [40], who presented a synthesis of underwater landforms and sediment types on the shelves surrounding the Iberian Peninsula and the Balearic Islands but did not attempt to quantify

the sediment thickness. There are other site-specific studies that provide local information about the sediment thickness and percentages of fines, sands, and gravels e.g., [28,41,42], but no study has been performed on the scale and resolution in this study. In this context, we have attempted to document, as clearly as possible, the datasets that we have used and the assumptions and simplifications made on each step. Both the STMA model produced and the QGIS tools used to extract the information from it have been made available via a publicly accessible repository. In this section, we summarize the main lessons learned during this study, and we enumerate several known limitations of the model in its present form:

- The baseline depth value chosen of 2050 m has implications in the results of sediment thickness values for the bottom layer, which, for this study, we have assumed is the consolidated gravel layer. The thickness of this layer is assumed to be the elevation difference between the modeled layer and the baseline, resulting in thickness values of the order of 2000 m, which is significantly larger than for the other five layers, whose values are of the order of 1 m to 100s m. This implies that the thickness value for the consolidated gravel layer needs to be interpreted differently than the others (e.g., volume calculations cannot be directly compared with the other five layers). A more accurate representation of the bottom layer will not be solved by using different base depths for the different sections but will require modeling the bedrock surface and resolving the vertical distribution of the different sediment fractions. The implications of the simulation of the coastal landscape evolution using CoastalME are minimal as this software includes, by default, the concept of the active layer via the definition of the availability factor, which assumes that gravel deposits are less available to be transported than sand and fine fractions.
- It is worth discussing the simplified hypothesis considered in the study. In general, the composition of the seabed can be well-described by the sequence of fine, sand, gravel, and unconsolidated and consolidated material, neglecting the above layers if the thickness is zero. However, some regions might be formed by a different sequence of sediment layers.
- The geological maps do not always match the same geological classification, e.g., in Huelva, sheet 998 has alphanumeric codes, e.g., QD for 'Holocene white sands' whereas sheet 1047 has numbered unit codes, e.g., 36 'Holocene sands, pebbles, and shells'. Also, a map unit code can have a different description on another sheet, e.g., QD is 'Holocene white sand' on sheet 998 and 'Aeolian sand' on 1033C. Regarding data management, it is worth mentioning the duplication of cross-sections in adjacent model areas and that Groundhog software v2.6 struggled to calculate some of the thickness models, so Huelva had to be split in two for explicit model calculation. In addition to this, it is difficult to keep track of inputting grain size/consolidation information into Groundhog. The model could be improved with more geological information such as boreholes, a shape file of the geology (the geology maps had to be geo-registered and digitized), and a stratigraphic order for the seabed sediments (a shape file showing their distribution was provided, but the stratigraphic order was inferred).
- The spatial scale can also be determinant in some regions. The cell size ranged between 25 and 100 m, which resulted in 5,601,683 cells for the Andalusian coastal zone. Even with that discretization, the spatial scale remains insufficient to model the cliffs that surround the coastline, e.g., in the eastern region of Almeria, where a successive sequence of small rocky coves shapes the coast. On the other hand, the methodology adequately represents the homogeneous sediment pattern of Huelva, Cádiz, and Málaga and the heterogeneity of the sediment of the beaches of Granada (G01 to G03).
- Finally, the queries and the model validation have highlighted the need to include the contribution made by rivers, especially if it is significant, as is the case with the Guadalquivir River. In the area of the large Andalusian rivers, and it likely will also be observed in the Guadiana (H01) and Tinto and Odiel in Huelva (H01 to H02), the

contributions that are given make the model differ significantly. Visual observations of the extent of the sediment plume make it evident that it is not being modeled correctly. Furthermore, the area of Almería (A01 to A06) and the east of Granada (G03) must have some geological layer in which attribution may significantly differ. Another notable aspect could be the incidence of contributions along the ramblas, which, during storm episodes, potentially move sediments of mean grain size that reach up to decimeters. That effect is potentially significant in Almería, where more than 30 ramblas split the coastline.

Coastal decision-makers now have an evidence-based model of the coastal zone that can be used to better manage the risk of coastal flooding and erosion. As shown by [43], a better quantification of the amount of unconsolidated material along the coast enables a better quantification of the level of protection offered against coastal erosion and interlinked coastal flooding. This allows the coastal stakeholder to define trigger points for interventions to ensure the minimum level of protection is secured. Projections of future changes in the coastal landscape from years to multiple decades are very sensitive to the assumed sediment thickness e.g., [13,44]. In the absence of sediment thickness information, the dominant assumption in most morphodynamic simulations is that sediment thickness is infinite (e.g., gradients on the littoral drift are not controlled by sediment availability). Our STMA model results clearly illustrate that this assumption is not applicable elsewhere along the Andalusian coastline. Even in the sand-rich coastal regions of Huelva (H01 and H02), the thickness of unconsolidated sand deposits is limited to 10s to 100s meters with high spatial variability along the coast.

The use of publicly accessible data and software proposed here will hopefully benefit the coastal engineering community, which can apply it to other locations. While Groundhog Desktop version v2.6, used in this study, is not freely available, the BGS Groundhog v2.8 is available under an Open Government Licence and is free to use for personal, educational, and commercial purposes. The functionalities used to generate the STMA are still available in Groundhog v2.8, and therefore, the methodology applied here is reproducible. We have also created a series of video tutorials explaining how to use GroundHog Desktop software v2.6 to create a STM (see Figure S2). The video tutorials are accessible via a GroundHog Desktop dedicated channel¹, where there is also a dedicated Coastal² playlist where we explain the different tasks for thickness modeling, setting up the software environment, creating boreholes, producing logs for CoastalME, creating sediment layers; sediment layers properties explained and exporting raster files. Both the STMA and the QGIS programs used to extract the information presented in this section are available in a publicly accessible repository.

Supplementary Materials: The following supporting information can be downloaded at: <https://www.mdpi.com/article/10.3390/jmse12020269/s1>, Figure S1. Cross-sections (in yellow) defined to explicit model in Groundhog desktop software over the STBM elaborated to use as input data; Figure S2. Screen capture showing the video tutorials explaining in detail how to use Groundhog Desktop to create Sediment Thickness Models for CoastalME applications.

Author Contributions: Conceptualization, A.P.; methodology, A.P.; software, C.T.; validation, C.T. and M.C.; formal analysis, A.P., M.C., H.B., D.M., H.S. and G.O.J.; investigation, A.P., M.C., H.B., D.M., H.S. and G.O.J.; resources, H.B. and C.T.; writing—original draft preparation, C.T., A.P., M.C. and H.B.; writing—review and editing, C.T., A.P., M.C., H.B. and G.O.J.; visualization, C.T. and H.B.; supervision, A.P.; project administration, A.P.; funding acquisition, A.P. All authors have read and agreed to the published version of the manuscript.

Funding: A.P.: G.O.J., H.B., D.M. and H.S. were funded by the CHAMFER project (NE/W004992/1).

Institutional Review Board Statement: Not applicable.

Informed Consent Statement: Not applicable.

Data Availability Statement: The data presented in this study are openly available in the Zenodo repository at <https://zenodo.org/>, with DOI [10.5281/zenodo.10284704].

Acknowledgments: A.P. acknowledges the contribution of Thomas Fletcher, who supported the modeling team in the use of GroundHog software and creating the video tutorials. The authors are grateful for the helpful comments of the three anonymous reviewers.

Conflicts of Interest: The authors declare no conflicts of interest.

Notes

- ¹ <https://www.youtube.com/@groundhogdesktop1075/featured>
- ² https://www.youtube.com/playlist?list=PLijTfdFfhXj6R-8FvFWSQB_WLAaqd1-xC

References

1. French, J.R.; Burningham, H. Coastal geomorphology: Trends and challenges. *Prog. Phys. Geogr. Earth Environ.* **2009**, *33*, 117–129. [[CrossRef](#)]
2. Burningham, H. Contrasting geomorphic response to structural control: The Loughros estuaries, northwest Ireland. *Geomorphology* **2008**, *97*, 300–320. [[CrossRef](#)]
3. Reeve, D.E.; Karunaratna, H.; Pan, S.; Horrillo-Caraballo, J.M.; Rózyński, G.; Ranasinghe, R. Data-driven and hybrid coastal morphological prediction methods for mesoscale forecasting. *Geomorphology* **2016**, *256*, 49–67. [[CrossRef](#)]
4. Noujas, V.; Thomas, K.V.; Badarees, K.O. Shoreline management plan for a mudbank dominated coast. *Ocean. Eng.* **2016**, *112*, 47–65. [[CrossRef](#)]
5. Mingle, J. *IPCC Special Report on the Ocean and Cryosphere in a Changing Climate*; 0028-7504; New York Review of Books: New York, NY, USA, 2020.
6. Wolinsky, M.A.; Murray, A.B. A unifying framework for shoreline migration: 2. Application to wave-dominated coasts. *J. Geophys. Res. Earth Surf.* **2009**, *114*, F01009. [[CrossRef](#)]
7. Shi, B.; Wang, Y.P.; Wang, L.H.; Li, P.; Gao, J.; Xing, F.; Chen, J.D. Great differences in the critical erosion threshold between surface and subsurface sediments: A field investigation of an intertidal mudflat, Jiangu, China. *Estuar. Coast. Shelf Sci.* **2018**, *206*, 76–86. [[CrossRef](#)]
8. Payo, A.; Williams, C.; Vernon, R.; Hulbert, A.G.; Lee, K.A.; Lee, J.R. Geometrical Analysis of the Inland Topography to Assess the Likely Response of Wave-Dominated Coastline to Sea Level: Application to Great Britain. *J. Mar. Sci. Eng.* **2020**, *8*, 866. [[CrossRef](#)]
9. Payo, A.; Favis-Mortlock, D.; Dickson, M.; Hall, J.W.; Hurst, M.D.; Walkden, M.J.A.; Townend, I.; Ives, M.C.; Nicholls, R.J.; Ellis, M.A. Coastal Modelling Environment version 1.0: A framework for integrating landform-specific component models in order to simulate decadal to centennial morphological changes on complex coasts. *Geosci. Model Dev.* **2017**, *10*, 2715–2740. [[CrossRef](#)]
10. Payo, A.; French, J.R.; Sutherland, J.; A Ellis, M.; Walkden, M. Communicating Simulation Outputs of Mesoscale Coastal Evolution to Specialist and Non-Specialist Audiences. *J. Mar. Sci. Eng.* **2020**, *8*, 235. [[CrossRef](#)]
11. Rattenbury, M.S.; Begg, J.G.; Jones, K.E.; Dabson, O.J.N.; Fitzgerald, R.J.; Payo, A.; Kessler, H.; Wood, B.; Burke, H.; Ellis, M.A.; et al. Application Theme 5—Geohazard and Environmental Risk Applications. In *Applied Multidimensional Geological Modeling*; John Wiley & Sons: Hoboken, NJ, USA, 2021; pp. 519–554.
12. Payo, A.; Walkden, M.; Ellis, M.; Barkwith, A.; Favis-Mortlock, D.; Kessler, H.; Wood, B.; Burke, H.; Lee, J. A quantitative assessment of the annual contribution of platform downwearing to beach sediment budget: Happisburgh, England, UK. *J. Mar. Sci. Eng.* **2018**, *6*, 113. [[CrossRef](#)]
13. Cobos, M.; Payo, A.; Favis-Mortlock, D.; Burke, H.; Morgan, D.; Jenkins, G.; Smith, H.; Fletcher, T.; Otiñar, P.; Magaña, P.; et al. Importance of Shallow Subsurface and Built Environment Characterization on Assessing Coastal Landscape Morphological Evolution from Hours to Decadal Time Scales: Application to Complex Landforms along Andalucía (Spain) Coastline. In Proceedings of the 39th IAHR World Congress, Granada, Spain, 22 June 2022.
14. Cobos, M.; Payo, A.; Favis-Mortlock, D.; Burke, H.; Morgan, D.; Jenkins, G.; Smith, H.; Fletcher, T.; Otiñar, P.; Magaña, P.; et al. Modelado de la morfología costera incluyendo elementos antrópicos y sustratos de distintos materiales. Aplicación a sistemas costeros complejos en un tramo del litoral granadino. In Proceedings of the XVI Jornadas Españolas de Ingeniería de Costas y Puertos, Vigo, Spain, 12 May 2022; p. 404.
15. Molina, R.; Anfuso, G.; Manno, G.; Gracia Prieto, F.J. The Mediterranean Coast of Andalusia (Spain): Medium-Term Evolution and Impacts of Coastal Structures. *Sustainability* **2019**, *11*, 3539. [[CrossRef](#)]
16. EEA. WFS Coastal Erosion Trends. 2015. Available online: http://data.adriplan.eu/geoserver/wfs?typename=geonode:erosion_trend&outputFormat=gml2&version=1.0.0&request=GetFeature&service=WFS (accessed on 29 January 2024).
17. Manno, G.; Anfuso, G.; Messina, E.; Williams, A.T.; Suffo, M.; Liguori, V. Decadal evolution of coastline armoring along the Mediterranean Andalusia littoral (South of Spain). *Ocean Coast. Manag.* **2016**, *124*, 84–99. [[CrossRef](#)]
18. Losada, M.; Baquerizo Azofra, A.; Ortega-Sánchez, M.; Ávila, A. Coastal Evolution, Sea Level, and Assessment of Intrinsic Uncertainty. *J. Coast. Res.* **2011**, *59*, 218–228. [[CrossRef](#)]
19. Wilkinson, M.D.; Dumontier, M.; Aalbersberg, I.J.; Appleton, G.; Axton, M.; Baak, A.; Blomberg, N.; Boiten, J.-W.; da Silva Santos, L.B.; Bourne, P.E.; et al. The FAIR Guiding Principles for scientific data management and stewardship. *Sci. Data* **2016**, *3*, 160018. [[CrossRef](#)]

20. Kessler, H.; Mathers, S.; Sobisch, H.-G. The capture and dissemination of integrated 3D geospatial knowledge at the British Geological Survey using GSI3D software and methodology. *Comput. Geosci.* **2009**, *35*, 1311–1321. [[CrossRef](#)]
21. BGS. BGS Groundhog v2.8. Available online: <https://www.bgs.ac.uk/technologies/software/groundhog/> (accessed on 29 January 2024).
22. INE. Demografía y Población. Available online: <https://www.ine.es/dynInfo/Infografia/Territoriales/capituloGraficos.html#!mapa> (accessed on 15 November 2023).
23. IECA. Directorio de Empresas y Establecimientos con Actividad Económica en Andalucía. 2021. Available online: <https://www.juntadeandalucia.es/institutodeestadisticaycartografia/direct/index.htm> (accessed on 29 January 2024).
24. IECA. Spatial Distribution of Andalusia Population. 2021. Available online: <https://www.juntadeandalucia.es/institutodeestadisticaycartografia/distribucionpob/index.htm> (accessed on 29 January 2024).
25. IECA. Encuesta de Coyuntura Turística de Andalucía 2022. Available online: <https://www.juntadeandalucia.es/institutodeestadisticaycartografia/turismo/index.htm> (accessed on 29 January 2024).
26. Morales, J.A. (Ed.) *The Spanish Coastal Systems. Dynamic Processes, Sediments and Management*, 1st ed.; Springer: Berlin/Heidelberg, Germany, 2019; p. 823.
27. Liqueste, C.; Arnau, P.; Canals, M.; Colas, S. Mediterranean river systems of Andalusia, southern Spain, and associated deltas: A source to sink approach. *Mar. Geol.* **2005**, *222–223*, 471–495. [[CrossRef](#)]
28. Jodar, J.M.; Voulgaris, G.; Luna del Barco, A.; Gutierrez-mas, J.M. Wave and Current Conditions and Implications for the Distribution of sediment in the Bay of Cadiz (Andalusia, SW Spain). In *Proceedings of the Litoral 2002, Porto, Portugal*, 22–26 September 2002.
29. Hearn, G.J. Geology, geomorphology and geohazards on a section of the Betic coastline, southern Spain. *Q. J. Eng. Geol. Hydrogeol.* **2019**, *52*, 208–219. [[CrossRef](#)]
30. IGN. Digital Terrain Model with 25-metre grid pitch (DTM25) of Spain. *MDT25*. 2015. Available online: <https://www.idee.es/csw-inspire-idee/srv/spa/catalog.search?#/metadata/spaignMDT25> (accessed on 29 January 2024).
31. Guisado, E.; Malvárez, G.C. Multiple Scale Morphodynamic mapping: Methodological Considerations and Applications for the Coastal Atlas of Andalusia. *J. Coast. Res.* **2009**, *56*, 1513–1517.
32. MMAA. Ecocartography of Cádiz, Málaga, Granada and Almería. *Ecocartography*. 2012. Available online: https://portalrediam.cica.es/descargas/index.php/s/mxHMWXYHfrCxyNK?path=/08_AMBITOS_INTERES_AMBIENTAL/02_LITORAL_MARINO/06_BATIMETRIAS (accessed on 29 January 2024).
33. EMODnet. DTM 2020. 2020. Available online: <https://emodnet.ec.europa.eu/en> (accessed on 29 January 2024).
34. CMAOT. Coastline 2013. 2013. Available online: https://portalrediam.cica.es/descargas/index.php/s/mxHMWXYHfrCxyNK?path=/08_AMBITOS_INTERES_AMBIENTAL/02_LITORAL_MARINO/02_GEOLOGIA/Linea_Costa_2013 (accessed on 29 January 2024).
35. IGME. Mapa Geológico de España a escala 1:50.000 (2ª Serie). *MAGNA50*. Available online: <http://info.igme.es/cartografiadigital/geologica/Magna50.aspx> (accessed on 29 January 2024).
36. IGME; IEO; Spanish-Universities. Geomorphologic Map of Spain and the Continental Margin at scale 1:1,000,000. 1979. Available online: https://portalrediam.cica.es/descargas/index.php/s/mxHMWXYHfrCxyNK?path=/08_AMBITOS_INTERES_AMBIENTAL/02_LITORAL_MARINO/02_GEOLOGIA/Geomorfologico_marino (accessed on 29 January 2024).
37. Barber, C.B.; Dobkin, D.P.; Huhdanpaa, H. The quickhull algorithm for convex hulls. *ACM Trans. Math. Softw.* **1996**, *22*, 469–483. [[CrossRef](#)]
38. QGIS.org. QGIS Geographic Information System. Open Source Geospatial Foundation. Available online: <https://qgis.org/> (accessed on 29 January 2024).
39. Serrano, M.A.; Díez-Minguito, M.; Ortega-Sánchez, M.; Losada, M.A. Continental shelf waves on the Alborán sea. *Cont. Shelf Res.* **2015**, *111*, 1–8. [[CrossRef](#)]
40. Fernández-Salas, L.M.; Durán, R.; Lobo, F.J.; Ribó, M.; Canals, M. Shelves of the Iberian Peninsula and the Balearic Islands (I): Morphology and sediment types. *Bol. Geol. Y Min.* **2015**, *126*, 327–376.
41. Gracia, F.-J.; Morales, J.-A.; Castañeda, C.; Plomaritis, T.A. Shallow lacustrine versus open ocean coastal clastic deposits: Morphosedimentary diagnostic indicators and interpretation. *Sediment. Geol.* **2021**, *423*, 105981. [[CrossRef](#)]
42. Jabaloy-Sánchez, A.; Lobo, F.J.; Azor, A.; Martín-Rosales, W.; Pérez-Peña, J.V.; Bárcenas, P.; Macías, J.; Fernández-Salas, L.M.; Vázquez-Vílchez, M. Six thousand years of coastline evolution in the Guadalfeo deltaic system (southern Iberian Peninsula). *Geomorphology* **2014**, *206*, 374–391. [[CrossRef](#)]
43. López, P.M.; Payo, A.; Ellis, M.A.; Criado-Aldeanueva, F.; Jenkins, G.O. A Method to Extract Measurable Indicators of Coastal Cliff Erosion from Topographical Cliff and Beach Profiles: Application to North Norfolk and Suffolk, East England, UK. *J. Mar. Sci. Eng.* **2020**, *8*, 20. [[CrossRef](#)]
44. Walkden, M.; Dickson, M. Equilibrium erosion of soft rock shores with a shallow or absent beach under increased sea level rise. *Mar. Geol.* **2008**, *251*, 75–84. [[CrossRef](#)]

Disclaimer/Publisher’s Note: The statements, opinions and data contained in all publications are solely those of the individual author(s) and contributor(s) and not of MDPI and/or the editor(s). MDPI and/or the editor(s) disclaim responsibility for any injury to people or property resulting from any ideas, methods, instructions or products referred to in the content.